Computation of Rotational Transonic Flows Using a Decomposition Method

K. Giannakoglou,* P. Chaviaropoulos,* and K. D. Papailiou†
Athens National Technical University, Athens, Greece

Any vector field may be decomposed, in a unique way, into an irrotational and a rotational part, if appropriate boundary conditions are imposed to the scalar and vector potentials introduced by the above decomposition. In the present work, the transformation is applied to the mass flux vector, in order to calculate two-dimensional, steady, rotational, transonic flows in arbitrarily shaped ducts and plane cascades. The whole procedure is discussed from an analytical and a numerical point of view, while finite difference-finite volume schemes are used to derive numerical results.

Nomenclature

a_1 = inlet flow angle
a_2 = outlet flow angle
c_p = specific heat at constant pressure
M = Mach number
n = outward normal to the boundary vector
p = pressure
R_g = universal gas constant
S = entropy
T = temperature
(u,v) = velocity components in (x,y) coordinate system
V = velocity vector
x,y = coordinates in physical space
γ = isentropic exponent
ξ,η = coordinates in computational space
ρ = density
Φ = scalar potential
Ψ = vector potential
ω = relaxation factor
Ω = vorticity

Subscripts and Superscripts

t = total thermodynamic quantities
n = normal to the boundary component
n = number of current iteration

(Note: Subscripting a variable with any of the coordinates indicates partial differentiation, whereas indices i,j indicate the node point.)

Introduction

DURING the past decade, quite a few methods have been developed for the calculation of the inviscid transonic flow. The existing computational methods for the steady two-dimensional rotational flows make use of the full Euler equations, numerically solved either directly by a time-marching technique[1,2] or through some convenient transformations leading to potential-type equations.

The Clebsch-type decomposition,[3] the velocity field analysis in terms of a scalar and a vector potential,[4] and the stream function formulation[5,6] are three well-known techniques, leading to an Euler equivalent system of second-order partial differential equations solved by fast iterative algorithms. Two remarkable advantages of the stream function formulation are the fast rate of convergence (because of the existing Dirichlet boundary conditions) and that of the method being conservative; whereas the main disadvantage is the nonunique determination of the static density in terms of the mass flux.

In contrast, direct solutions of the Eulerian primary variables system are time-consuming when compared to a potential-type computation, whereas entropy losses, introduced by the necessary artificial dissipation schemes, are not controllable.

In this work, the decomposition of the mass flux vector field into irrotational and solenoidal components is used, while an appropriate set of boundary conditions is chosen to assure the uniqueness of the transformation. A novel explicit iterative scheme is proposed in order to overcome the double root difficulty of the mass flux density relation. The rotationality is introduced by nonuniform stagnation conditions at the channel entrance, and the vorticity is evaluated according to Crocco's theorem.

Finite difference-finite volume schemes are used to discretize the partial differential equations, and computations are performed for various two-dimensional, subsonic and transonic, inviscid flows in ducts or cascades. An artificial density term is activated in the supersonic region of a mixed-type flow to capture the shock wave and assure the convergence of the algorithm.

Governing Equations

Our analysis is based on the decomposition[7] of the ρV vector field into an irrotational and a solenoidal part expressed as

$$\rho V = \nabla\Phi + \nabla \times \Psi \tag{1}$$

For a Cartesian coordinate system (x, y), the ρV components corresponding to Eq. (1) can be written as

$$\rho u = \Phi_x + \Psi_y \tag{2a}$$

$$\rho v = \Phi_y - \Psi_x \tag{2b}$$

The mass conservation and the vorticity definition give

$$\Phi_{xx} + \Phi_{yy} = 0 \tag{3}$$

$$\left(\frac{1}{\rho}\Psi_x\right)_x + \left(\frac{1}{\rho}\Psi_y\right)_y = -\Omega + \left(\frac{1}{\rho}\Phi_y\right)_x - \left(\frac{1}{\rho}\Phi_x\right)_y \tag{4}$$

Received May 22, 1986; revision received Nov. 21, 1987.

*Research Scientist.
†Professor, Laboratory of Thermal Turbomachines. Member AIAA.

where Ψ represents the $\boldsymbol{\Psi}$ component that is normal to the flow plane.

According to Crocco's theorem,[8] the vorticity Ω can be expressed in terms of the thermodynamic properties of the fluid:

$$\frac{\Omega}{\rho} = \frac{1}{\rho \boldsymbol{V} \cdot \boldsymbol{u}_1} \left\{ \left[\frac{1}{\gamma} \left(\frac{\rho}{\rho_t} \right)^{\gamma - 1} - 1 \right] c_p \frac{\partial T_t}{\partial \boldsymbol{u}_2} - R_g \left(\frac{\rho}{\rho_t} \right)^{\gamma - 1} \frac{T_t}{\rho_t} \frac{\partial \rho_t}{\partial \boldsymbol{u}_2} \right\} \tag{5}$$

where $\boldsymbol{u}_1$ and $\boldsymbol{u}_2$ are two perpendicular unit vectors.

Assuming an adiabatic and inviscid flow, the governing equations

$$\rho u (T_t)_x + \rho v (T_t)_y = 0 \tag{6}$$

$$\rho u (\rho_t)_x + \rho v (\rho_t)_y = 0 \tag{7}$$

imply that the stagnation quantities are conserved along the streamlines. In the present state of this work, the entropy increase across the shock wave is not taken into account, and the corresponding vorticity variation introduced behind the shock is thus neglected.

The system of equations is completed by the equation

$$\left(\frac{\rho}{\rho_t} \right)^{\gamma - 1} + \frac{V^2}{2 c_p T_t} = 1 \tag{8}$$

Boundary Conditions

The scalar potential Φ, governed by Eq. (3), is specified to have as boundary conditions

$$\boldsymbol{n} \cdot \nabla \Phi = \Phi_n = \rho \boldsymbol{V} \cdot \boldsymbol{n} \tag{9}$$

The requirement that $\boldsymbol{\Psi}$ must be solenoidal ($\nabla \cdot \boldsymbol{\Psi} = 0$) for a two-dimensional flow problem may be expressed at the boundary as

$$\Psi = 0 \tag{10}$$

which constitutes the boundary condition on the vector potential differential Eq. (4). This set of boundary conditions proposed by Hirasaki and Hellums[9,10] assures the uniqueness of transformation of Eq. (1). Applying the following transformation

$$\frac{\partial \Phi^*}{\partial x} = -\frac{\partial \Phi}{\partial y}, \qquad \frac{\partial \Phi^*}{\partial y} = \frac{\partial \Phi}{\partial x}$$

onto the Laplace-type Eq. (3) with Neumann boundary conditions, Eq. (9), our problem can be reduced to a Dirichlet Laplacian one assuming a faster rate of convergence. The whole set of boundary conditions, which have to be prescribed, consists on the mass flux ($\rho \boldsymbol{V} \cdot \boldsymbol{n}$) distribution at the entrance and the exit of the duct, as well as the stagnation density and temperature distributions at the entrance. There is no mathematical restriction covering the kinematic and aerodynamic quantities at the entrance, but care must be taken to avoid nonphysical angles of attack or radii of curvature. The vorticity distribution is not given as inlet boundary condition but can be evaluated through Eq. (5), considering as $\boldsymbol{u}_2$ the unit vector tangent to the entrance boundary.

When dealing with a plane cascade flow, a different set of boundary conditions is applied, including the known values of the inlet and outlet flow angles and the periodicity condition, which is valid on any set of corresponding periodic boundary nodes.

Coordinate Transformation

A transformation from the physical plane (x,y) to the computational plane (ξ,η), resulting in a rectangular computational grid, has been used. This technique allows arbitrary spacing of points along the boundary and provides greater accuracy, since equally spaced mesh points are used in the computational plane. Thus, the presence of irregular boundary shapes in the physical plane can be easily handled.

A Laplacian coordinate transformation[11] is used in most cases in this work, namely,

$$\xi_{xx} + \xi_{yy} = 0 \tag{11a}$$

$$\eta_{xx} + \eta_{yy} = 0 \tag{11b}$$

Arbitrary grids are used, though, if the above-mentioned transformation cannot describe adequately the physical situation at hand. Examples of both types of transformation will be presented in the context of the present work.

The expression of Eqs. (3) and (4) in the computational plane is

$$[(1/J)(A_1 \Phi_\xi + A_2 \Phi_\eta)]_\xi + [(1/J)(A_2 \Phi_\xi + A_3 \Phi_\eta)]_\eta = 0 \tag{12}$$

$$[(1/\rho J)(A_1 \Psi_\xi + A_2 \Psi_\eta)]_\xi + [(1/\rho J)(A_2 \Psi_\xi + A_3 \Psi_\eta)]_\eta = (1/J) F(\Omega, \rho, \Phi) \tag{13}$$

where

$$A_1 = \xi_x^2 + \xi_y^2 \tag{14a}$$

$$A_2 = \xi_x \eta_x + \xi_y \eta_y \tag{14b}$$

$$A_3 = \eta_x^2 + \eta_y^2 \tag{14c}$$

$$J = \xi_x \eta_y - \xi_y \eta_x \tag{14d}$$

$$F(\Omega, \rho, \Phi) = -\Omega + [(1/\rho)\Phi_y]_x - [(1/\rho)\Phi_x]_y \tag{14e}$$

Calculation Procedure

To solve numerically Eqs. (2–8), the following iterative procedure is followed:

Step 1: Solve Eq. (3) for Φ. Thus, an initial incompressible, irrotational flowfield can be calculated, if

$$\rho u = \Phi_x, \qquad \rho v = \Phi_y$$

This equation is solved once.

Step 2: Having the velocity field, calculate the position of a set of streamlines and transport the stagnation thermodynamics quantities T_t and ρ_t along them.

Step 3: Determine the vorticity field through Eq. (5).

Step 4: Calculate the static density distribution through Eq. (8) and apply the artificial density scheme.

Step 5: Estimate the rotational field, solving Eq. (4) and determine the total velocity distribution, using Eq. (2).

Step 6: Repeat Steps (2–6) until a satisfactory convergence is obtained.

Numerical Analysis

Partial Differential Equations

Since Eq. (12) is, mathematically speaking, a special form of the vector potential Eq. (13), only the later one will be discussed.

The following equation is an equivalent form of Eq. (13), namely,

$$a_1 \Psi_{\xi\xi} + a_3 \Psi_{\eta\eta} + 2a_2 \Psi_{\xi\eta} + a_4 \Psi_\xi + a_5 \Psi_\eta = (1/J) F(\Omega, \rho, \Phi) \tag{15a}$$

$$a_1 = A_1/\rho J, \quad a_2 = A_2/\rho J, \quad a_3 = A_3/\rho J$$

$$a_4 = (a_1)_\xi + (a_2)_\eta, \quad a_5 = (a_2)_\xi + (a_3)_\eta \tag{15b}$$

Equation (15) is discretized in central finite differences of the second order in the computational plane, where the grid points are equally spaced ($\Delta\xi = \Delta\eta = 1$). The numerical solution has been obtained using three different numerical procedures:

1) Given a successive overrelaxation method (SOR) with an optimum-computed relaxation factor equal to $\omega = 1.75$, the applied scheme is the following:

$$\Psi_{j,l}^{(n+1)} = (1-\omega)\Psi_{j,l}^{(n)} + \omega\tilde{\Psi}_{j,l}$$

$$2(a_1+a_3)\tilde{\Psi}_{j,l} = -\frac{1}{J}F_{j,l}^{(n)} + \left(a_1 + \frac{a_4}{2}\right)\Psi_{j+1,l}^{(n)} + \left(a_1 - \frac{a_4}{2}\right)\Psi_{j-1,l}^{(n+1)} + \left(a_3 + \frac{a_5}{2}\right)\Psi_{j,l+1}^{(n)} + \left(a_3 - \frac{a_5}{2}\right)\Psi_{j,l-1}^{(n+1)} + \frac{a_2}{2}[\Psi_{j+1,l+1}^{(n)} + \Psi_{j-1,l-1}^{(n+1)} - \Psi_{j+1,l-1}^{(n)} - \Psi_{j-1,l+1}^{(n+1)}]$$

2) A successive line overrelaxation method (SLOR) leads to the following system of equations solved for each vertical line $j = \text{const}$:

$$\left(a_3 + \frac{a_5}{2}\right)\Psi_{j,l+1}^{(n+1)} + \left(a_3 - \frac{a_5}{2}\right)\Psi_{j,l-1}^{(n+1)} - 2\omega(a_1+a_3)\Psi_{j,l}^{(n+1)} = (1/J)F_{j,l}^{(n)} - a_1[\Psi_{j+1,l}^{(n)} - 2(1-\omega)\Psi_{j,l}^{(n)} + \Psi_{j-1,l}^{(n+1)}] + 2a_3(1-\omega)\Psi_{j,l}^{(n)} - \frac{a_2}{2}[\Psi_{j+1,l+1}^{(n)} + \Psi_{j-1,l-1}^{(n+1)} - \Psi_{j+1,l-1}^{(n)} - \Psi_{j-1,l+1}^{(n+1)}] - \frac{a_4}{2}[\Psi_{j+1,l}^{(n)} - \Psi_{j-1,l}^{(n+1)}]$$

An underrelaxation factor of the order of 0.90 seems to give the best results.

3) Following an Alternating Direction Implicit[12] method (ADI), Eq. (15) may be written in the form of an operator $L(\Psi)$, namely,

$$L(\Psi) = a_1\Psi_{\xi\xi} + a_3\Psi_{\eta\eta} + 2a_2\Psi_{\xi\eta} + a_4\Psi_{\xi} + a_5\Psi_{\eta} - (1/J)F(\Omega,\rho,\Phi) = 0$$

Thus, introducing the residual $\Delta\Psi^{(n)}$,

$$\Delta\Psi_{j,l}^{(n)} = \Psi_{j,l}^{(n+1)} - \Psi_{j,l}^{(n)}$$

the iterative solution of the following scheme is required:

$$N\Delta\Psi^{(n)} = a\omega L(\Psi)$$

where

$$N = [a - a_1\delta_{\xi\xi}][a - a_3\delta_{\eta\eta}]$$

and $\alpha, \omega = \text{const}$.

To obtain the $\Psi^{(n+1)}$ value, a two-step procedure has been used, namely,

First step:

$$[a - a_1\delta_{\xi\xi}]f^{(n)} = a\omega L(\Psi)^{(n)}$$

Second step:

$$[a - a_3\delta_{\eta\eta}]\Delta\Psi^{(n)} = f^{(n)}$$

$$\Psi^{(n+1)} = \Psi^{(n)} + \Delta\Psi^{(n)}$$

The values $\alpha = 0.11$ and $\omega = 1.85$ have been successfully used.

Static Density-Mass Flux Relation

Equation (8) leads to the density-mass flux relation

$$A(\rho/\rho_t)^{-2} + (\rho/\rho_t)^{\gamma-1} = 1 \tag{16}$$

where

$$A = \frac{(\rho V)^2}{2c_p T_t \rho_t^2}$$

Equation (16) accepts two discrete roots for the static-total density ratio (ρ/ρ_t), corresponding to the subsonic and supersonic case. In order to circumvent the double root difficulty, two numerical expressions for Eq. (16) have been tested, namely,

$$(\rho/\rho_t)^{\nu+1} = \{1 - A[(\rho/\rho_t)^{\nu}]^{-2}\}^{1/\gamma-1} \tag{17a}$$

$$(\rho/\rho_t)^{\nu+1} = \sqrt{A}\{1 - [(\rho/\rho_t)^{\nu}]^{\gamma-1}\}^{-1/2} \tag{17b}$$

Applying Eq. (17a) or (17b) iteratively inside Step 4 of the above-mentioned algorithm, it was possible to obtain solutions even for high subsonic flowfields. We found that it was possible to extend our calculation to the transonic regime, applying Eq. (17a) once during each fourth step of the algorithm, modifying in parallel the computed density values in the supersonic regime through an artificial density scheme. A monotonic convergence was obtained in this way for all calculations per-

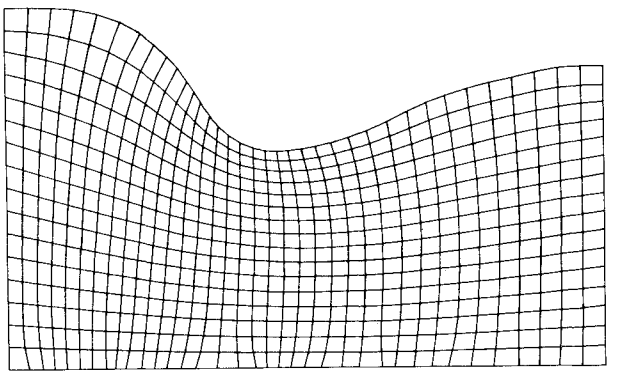

a) Convergent-divergent nozzle

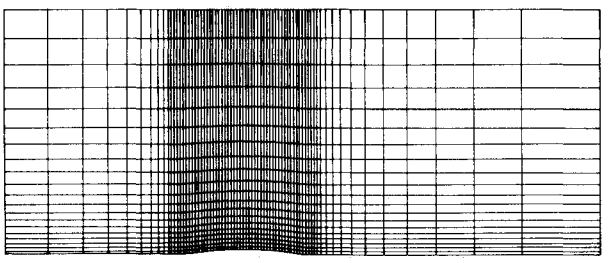

b) Parallel channel with a bump

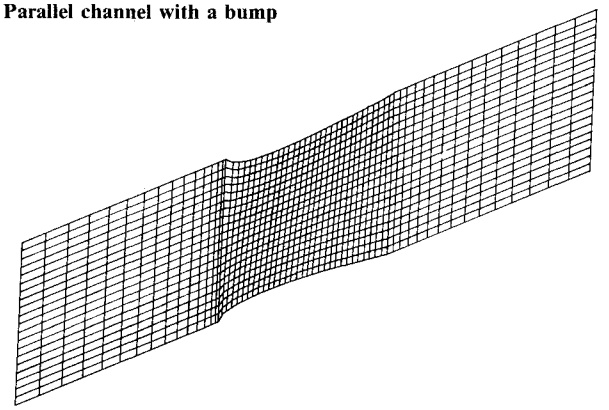

c) Cascade of NACA 0012 airfoils

Fig. 1 Computational domains and meshes.

formed. A similar density algorithm applied to transonic, mildly rotational, implicit scheme calculations has been used lately.[5,6]

Artificial Density Scheme

Artificial viscosity is added to the flow through the following artificial density scheme:[13]

$$\rho = \rho - \mu \frac{\tilde{\delta}\rho}{\partial s} \Delta \tag{18}$$

where $\tilde{\delta}/\partial s$ denotes upstream derivatives.

The switching function μ is activated in the supersonic regime, according to the expression

$$\mu = K \cdot \max\left(0, 1 - \frac{M_c^2}{M^2}\right) \tag{19}$$

The values $K = 1$ and $M_c = 1$ are currently used.

Transfer of Thermodynamic Quantities

The direct numerical solution of Eqs. (6) and (7) is particularly time-consuming in the absence of diffusion terms. Therefore, an alternative procedure has been used, which is based on the conservation of the total density and the total temperature along streamlines, once these lines have been located. This is done through a mass flow rate integration along each normal $\xi = \text{const}$, so that individual stream tubes may be isolated.

Results and Discussions

Several computations were performed, including cases of potential and rotational flows in arbitrarily shaped ducts or plane cascades, using the procedure described above. The test geometries, presented in Fig. 1, are: 1) a Laval-type convergent-divergent nozzle with an outlet-to-inlet cross-section area ratio of 0.83 [a Laplacian mesh of (37 × 17) grid points was used]; 2) a parallel channel having a 4.2% thick circular arc "bump" on the lower wall [an arbitrary mesh of (72 × 21) grid points was used]; and 3) a 25 deg staggered cascade of NACA 0012 airfoils with a pitch-to-chord ratio of 0.896 [the inlet-outlet flow conditions were $M_{in} = 0.69$, $a_1 = 25$ deg, and $a_2 = 25$ deg, and a linear (62 × 21) grid was used].

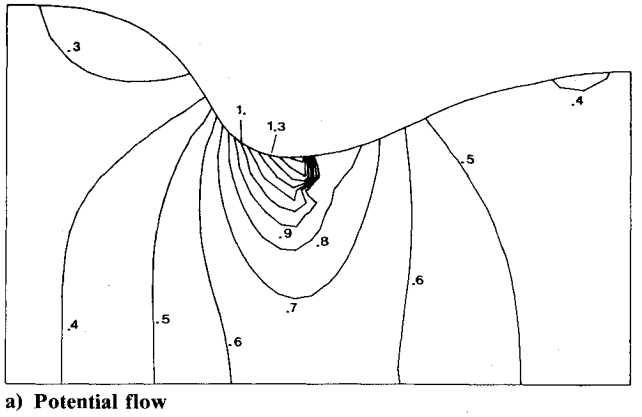

a) Potential flow

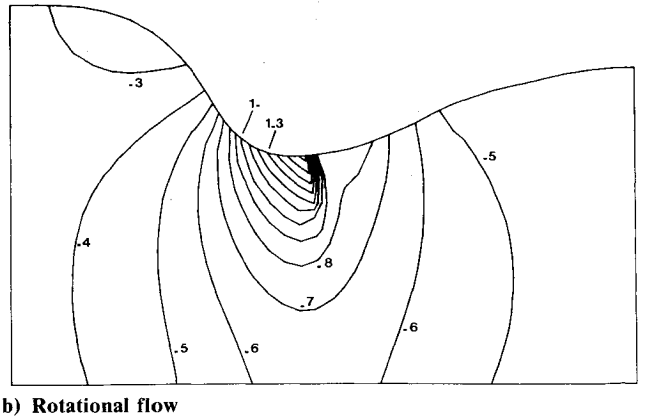

b) Rotational flow

Fig. 2 Mach number contours.

The computational algorithm was programmed in Fortran IV language for a CDC 171-8 computer, and the corresponding code was developed for an arbitrary grid. For both potential and rotational flows, uniform mass flux distributions at inlet and outlet and uniform total density distribution at inlet were imposed. For potential flows the total temperature distribution at inlet was taken to be uniform, whereas for rotational cases, rotationality was introduced by a linear distribution of T_t at the entrance.

For the solution of the Poisson-type equations, the following convergence criterion was used:

$$\max|(\Psi^{n+1} - \Psi^n)/\Psi^n| < 10^{-6} \tag{20}$$

which was assumed to be a sufficiently strict one.

Assuming that convergence of the complete algorithm is satisfactory when

$$\max|[(\rho V)^{N+1} - (\rho V)^N]/(\rho V)^N| < 10^{-3} \tag{21}$$

it was found that the necessary number of iterations was no more than 12 for the high-subsonic case and no more than 25 for cases where a strong shock was present in the passage. In Eqs. (20) and (21), the index n stands for the iteration number during solution of Eq. (3) on Φ (Step 1), or Eq. (4) on Ψ (Step 5), whereas the index N stands for the "external" iteration number (successive execution of Step 2 to Step 6). Rotationality does not seem to affect the convergence characteristics of the algorithm. On the contrary, we have observed that sometimes it facilitates convergence in transonic flow cases. Figure 2 presents the Mach number field issued from the computation of the flow through the Laval-type nozzle case. One may remark the differences present between the potential flow solution and the rotational one, which was obtained for a linear variation of the total temperature distribution at the inlet.

Figures 3 and 4 present results for the parallel channel with the bump case. This is a GAMM workshop case, for which the inlet Mach number was given equal to 0.85. The results presented in Figs. 3 and 4 were obtained for an inlet Mach number of 0.8245. No converged solution was possible above this Mach number. Jameson[14] reports similar difficulties with his transonic full potential code and attributes them to the fact that the Mach number value of 0.85 corresponds to a purely isentropic flow.

In Fig. 4 our results are compared with those of Deconinck and Hirsch.[15] Slight differences may be attributed to the difference existing in the value of the inlet Mach number that was used.

Figure 5 presents the Mach number field for the NACA 0012 cascade case.

Figure 6 gives a comparison between our results and those obtained by Habashi and Hafez.[5] The two methods give identical results for the pressure side, whereas for the suction side

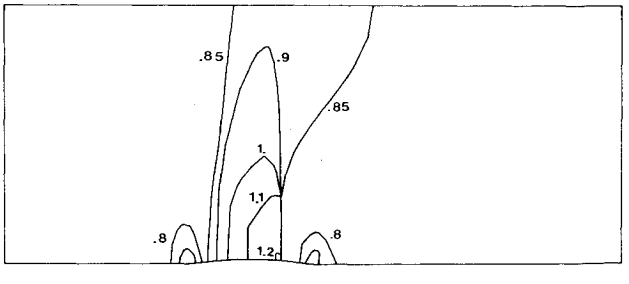

Fig. 3 Mach number contours.

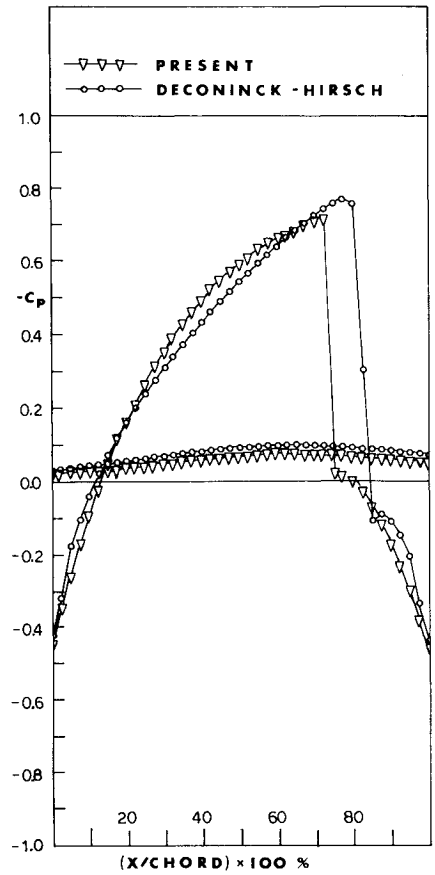

Fig. 4 Pressure coefficient distribution for the bump case.

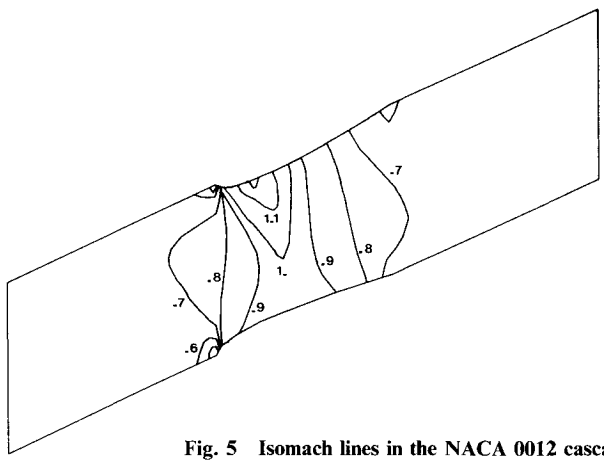

Fig. 5 Isomach lines in the NACA 0012 cascade.

slight differences are present. It must be noted that the artificial density scheme used was different and that the finite-element grid was coarser than ours.

Different iterative schemes were used to obtain numerical results. We can, generally, report that the SOR and SLOR schemes were found more effective for meshes containing less than, roughly, 1000 grid points, whereas for larger meshes the ADI method was found to be more economic. An interesting feature of the method is that the shock wave is located always between two successive grid points. We may speculate about the reasons leading to this fact, but no satisfactory explanation has been found up to now.

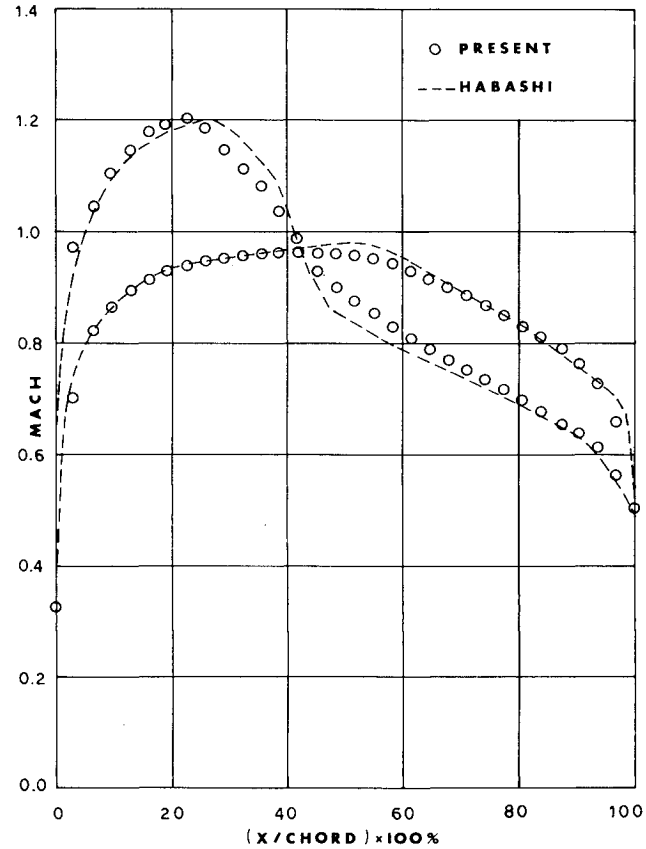

Fig. 6 Mach number distribution on the solid walls of the NACA 0012 cascade.

Conclusions

A method has been presented for numerically solving the two-dimensional, transonic, strongly rotational, inviscid flow problems inside ducts of arbitrary shape.

The rotationality was introduced by a nonuniform distribution of the total thermodynamic quantities at the entrance, and the vorticity generation behind the shock was, in the present form of the work, neglected.

Care was taken to conserve the mass flux (acting upon the product ρV rather than the velocity vector V) and to avoid solving directly the Euler equations, transporting instead total quantities along streamlines, which may be located easily and accurately.

An efficient method was developed for distinguishing the two branches, subsonic and supersonic, so that numerically speaking, the problem was reduced into solving a Poisson-type equation with Dirichlet boundary conditions.

Unlike previous workers[6,16] who have adopted an implicit algorithm to solve the equations of motion, combining it with an equation for the calculation of the static density, a semi-explicit technique was used [solution of Eqs. (4) and (8)]. The main advantages of the present formulation came out to be the reduced computer time required for rotational flow computations, the possibility to handle flows with shock waves blocking the complete passage as well as incompressible ones, and the fact that the captured shock wave is never smeared, being always located between two successive grid points of the mesh.

Acknowledgments

The authors would like to thank the Sté Avions Marcel Dassault-Brequet Aviation for stimulating and partially funding this research.

References

[1]Sod, G. A., "A Survey of Several Finite Difference Methods for Systems of Nonlinear Hyperbolic Conservation Laws," *Journal of*

Computational Physics, Vol. 27, Oct. 1978, pp. 1–31.

[2]Oliver, O. A. and Sparis, P., "A Computational Study of Three-Dimensional Shear Flow in Turbomachine Cascades," AIAA Paper 71-83, 1983.

[3]Ecer, A. and Acay, H. U., "A Finite Element Formulation of Euler Equations for the Solution of Steady Transonic Flows," AIAA Paper 82–0062, Jan. 1982.

[4]Sokhey, J. S., "Transonic Flow Around Axisymmetric Inlets Including Rotational Flow Effects," AIAA Paper 80–0341, Jan. 1980.

[5]Habashi, W. G. and Hafez, M., "Finite Element Stream Function Solutions for Transonic Turbomachinery Flows," AIAA Paper 82–1268, June 1982.

[6]Hafez, M. and Lovell, D., "Numerical Solution of Transonic Stream Function Equation," *AIAA Journal*, Vol. 21, March 1983, pp. 327–335.

[7]Aris, R., *Vectors, Tensors and the Basic Equations of Fluid Mechanics*, Prentice-Hall, Englewood Cliffs, NJ, 1962.

[8]Serrin, J., "Mathematical Principles of Classical Fluid Mechanics," *Encyclopedia of Physics*.

[9]Hirasaki, G. J. and Hellums, J. D., "A General Formulation of the Boundary Conditions on the Vector Potential in Three-Dimensional Hydrodynamics," *Quarterly of Applied Mathematics*, Vol. 16, 1968, pp. 331–342.

[10]Hirasaki, G. J. and Hellums, J. D., "Boundary Conditions on the Vector and Scalar Potentials in Viscous Three-Dimensional Hydrodynamics," *Quarterly of Applied Mathematics*, Vol. 28, 1970, pp. 293–296.

[11]Thomson, F. J., "Numerical Solution of Flow Problems Using Body-Fitted Coordinate Systems," *Computational Fluid Dynamics*, VKI Book, 1980.

[12]Baker, T., "The Computation of Transonic Potential Flow," *Computational Fluid Dynamics*, VKI LS 1981–05.

[13]Holst, L. T., "A Fast, Conservative Algorithm for Solving the Transonic Full-Potential Equation," American Society of Mechanical Engineers, Paper 79–1456.

[14]Jameson, A., Caughey, D., Jon, W., and Steinhoff, J., "Accelerated Finite-Volume Calculation of Transonic Potential Flows," *Numerical Methods for the Computation of Inviscid Transonic Flows with Shock Waves*, F. Vieweg, 1981.

[15]Deconinck, H. and Hirsch, C., "Transonic Flow Computations with Finite Elements," *Numerical Methods for the Computation of Inviscid Transonic Flows with Shock Waves*, F. Vieweg, 1981.

[16]Brown, E. F., Brecht, T. J. F., and Walsh, K. E., "A Relaxation Solution of Transonic Nozzle Flows Including Rotational Flow Effects," *Journal of Aircraft*, Vol. 14, Oct. 1977, pp. 944–951.